ELECTRONIC SUPPORTING INFORMATION

An Unprecedented Double Photoexcitation Mechanism for Photoswitching in Conjugated-Dienes to Trigger Physiological Processes for Photopharmacology

Akanksha Ashok Sangolkar, Rama Krishna Kadiyam, and Ravinder Pawar*

Laboratory of Advanced Computation and Theory for Materials and Chemistry, Department of Chemistry, National Institute of Technology Warangal (NITW), Warangal, Telangana-506004, India.

ravinder_pawar@nitw.ac.in

TABLE OF CONTENTS

S I. Computational details for *in silico* molecular docking simulations

The co-crystallized ligand was initially removed from the internal cavity of the β-barrel protein and thereafter all the bound water molecules were deleted from the crystal structure. Polar hydrogens and charges were subsequently added to the receptor protein structure *en route* to facilitate *in silico* molecular docking simulations. A sampling box with dimensions of 40x40x40 along the three axes and grid spacing of 0.375 was centered at 27.701, 19.236, and 48.968. The molecular docking simulations were conducted using AutoDock Vina and the results were visualized and analysed *via* AutoDockTools and Protein-Ligand Interaction Profiler.[1–3]

S II. Molecular structure and optimised geometries

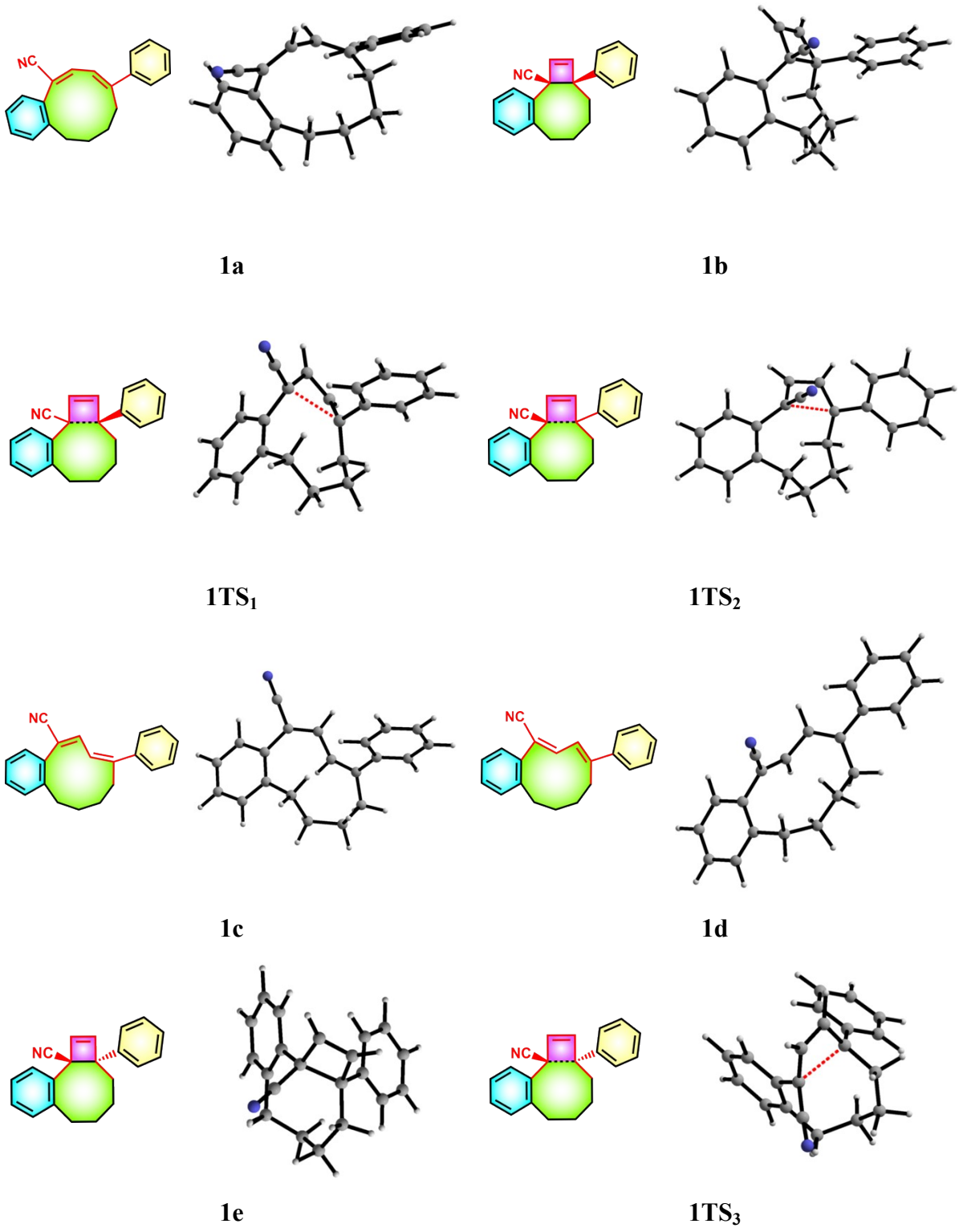

Figure S1. Molecular structure and the optimized geometry of the stationary and saddle point structures obtained during the photoswitching of the studied cyclic conjugated-diene. (M06-2X/Def2TZVP)

S III. Spectral data of photoisomers (TD-M06-2X/Def2TZVP).

Table S1. Calculated spectral data of photoisomers obtained during the 4π-electrocyclization based photoswitching cycle in studied substituted cyclodeca-1,3-diene in the gas phase and in the presence of water.

System	λ_{onset} (nm)	λ (nm)	*f*	ε (LM^{-1})	Transition and transition coefficient
			Gas phase		
1a	323.6	255.47	0.2686	10989.00	H→L (0.669)
		222.77	0.1372	12821.03	H→L+1 (0.498), H-2→ L (0.333)
		186.63	0.2407	24426.04	H-1→L+1 (0.346), H-2→L+1 (0.335), H-3→L (0.215)
1b	242.0	188.03	0.4917	64984.27	H→L (0.377), H-1→L+1 (0.287), H-3→L+1 (0.224), H→L+1 (0.221)
1c	388.8	288.77	0.5907	19978.48	H→L (0.697)
		206.10	0.1012	14791.20	H→L+4 (0.591)
		196.69	0.1353	17674.68	H-5→L (0.324), H→L+3 (0.222), H-6→L (0.215), H-1→L+3 (0.215), H-1→L+1 (0.204)
1d	335.6	263.62	0.2414	9211.27	H→L (0.667)
		226.60	0.2699	13467.92	H→L+1 (0.600)
		187.46	0.2816	19164.28	H-2→L+1 (0.316), H→L+5 (0.27126), H-2→L+4 (0.256), H-2→ L+3 (0.254), H-5→L (0.209)
1e	251.0	193.09	0.2344	29402.34	H-2→L+1 (0.361), H-2→L (0.261), H→L+1 (0.225), H→L (0.201)
			In water		
1a	353.8	269.04	0.5857	22857.21	H→L (0.667)
		237.82	0.2092	28268.98	H→L+1 (0.490), H-3→L+1 (0.256), H→L+4 (0.247)
		207.18	0.6754	81394.20	H→L+4 (0.383), H-3→L+1 (0.352), H-3→L (0.289)
1b	265.4	198.60	1.1149	143220.60	H-1→L (0.352), H-2→L+3 (0.334), H→L+1 (0.200)
1c	444.4	313.73	1.0161	34287.15	H→L (0.696)
		221.59	0.3046	43123.21	H→L+2 (0.407), H-4→ L (0.335), H-1→L (0.281)
		204.20	0.5505	58483.75	H-1→L+2 (0.444), H-1→L+1 (0.365), H-1→L+3 (0.250)
1d	504.4	341.41	1.1541	38917.22	H→L (0.697)

		221.60	0.3470	37312.89	H-4→L (0.462), H→L+4 (0.303), H→L+1 (0.242)
		202.07	0.4636	52583.73	H-1→L+3 (0.371), H-1→L+2), H-1→L+4 (0.204)
1e	269.6	196.26	0.9206	122478.66	H-3→L+1 (0.324), H-2→L+3 (0.271), H-2→L+1 (0.261)

S IV. Intrinsic reaction coordinates (IRC) profiles

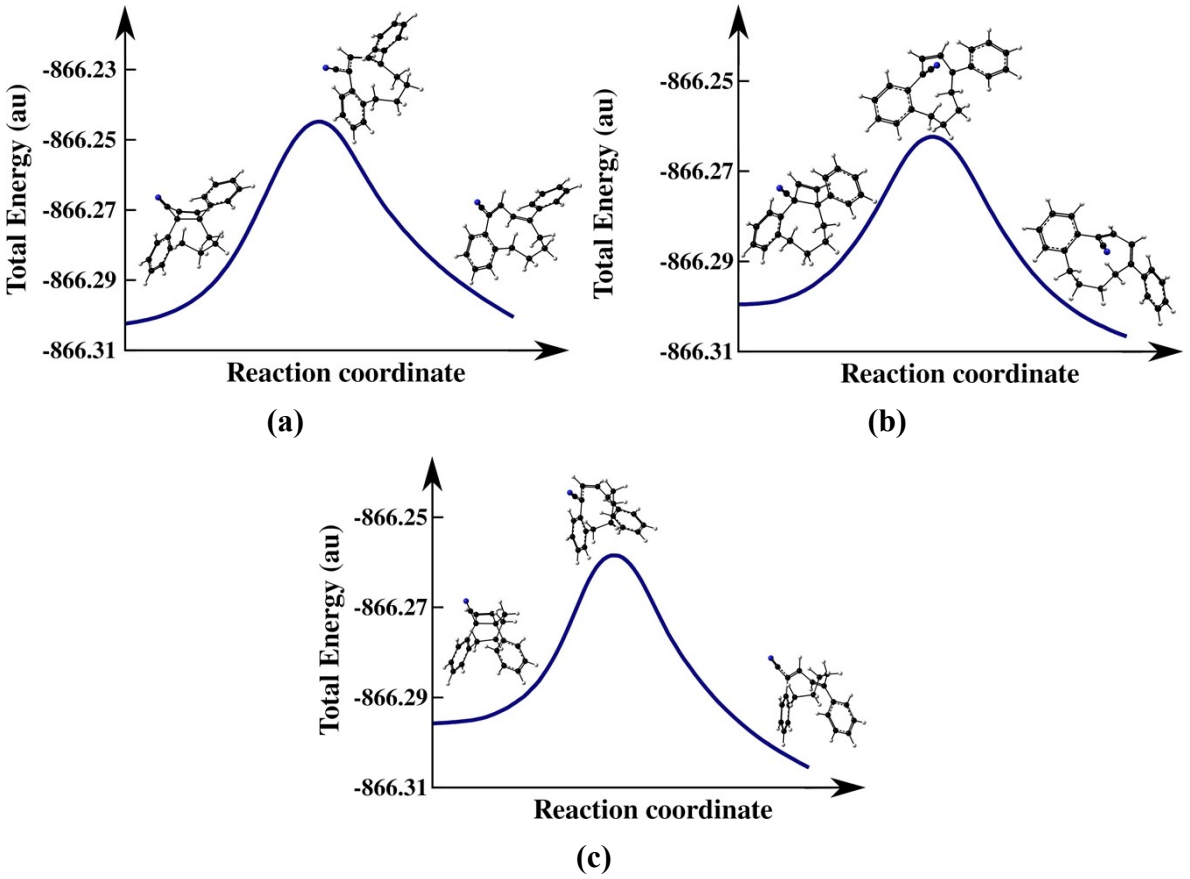

Figure S2. Intrinsic reaction coordinates (IRC) profiles for the thermal electrocyclic ring opening of fused bicyclobutene to cCDs. **(a)** Conversion of *cis*-bicyclobutene **1b** to *cis*,*trans*-cCD **1c**, (b) transformation of *cis*-bicyclobutene **1b** to *cis*,*trans*-cCD **1d**, and (c) thermolysis of *cis*-bicyclobutene **1e** to *cis*,*trans*-cCD **1a**.

S V. Intrinsic bond orbital (IBO) analysis

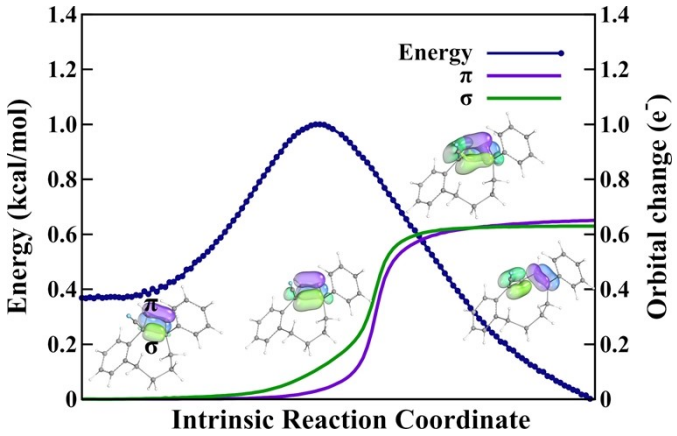

Figure S3. Change in actively participating intrinsic bond orbitals (IBOs) during the thermal electrocyclic ring opening of *cis*-bicyclobutene **1b** to *cis*,*trans*-cCD **1d**.

S VI. Reaction energetics, rate constant and half-lives

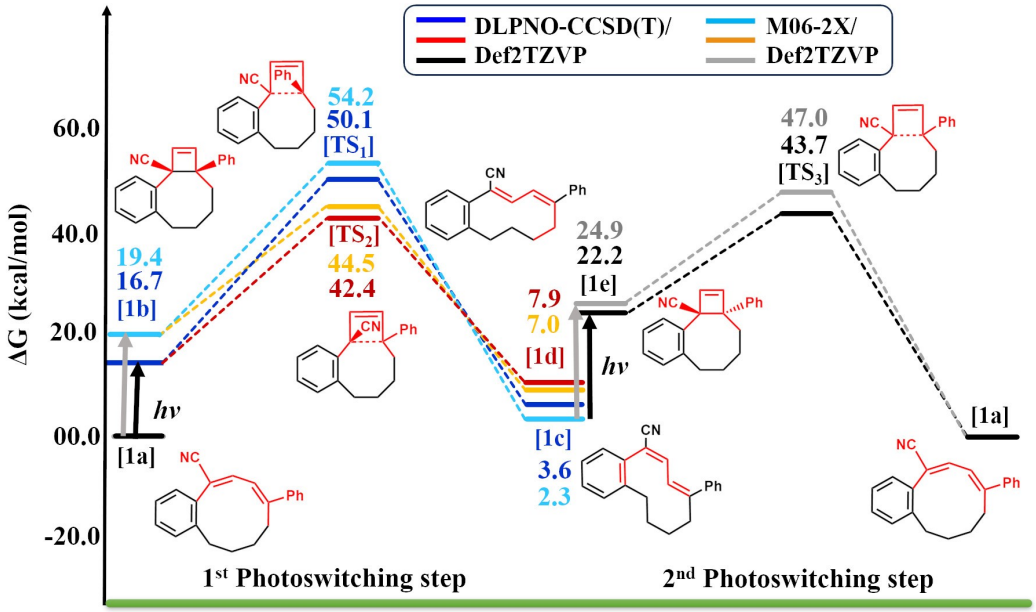

Gas phase

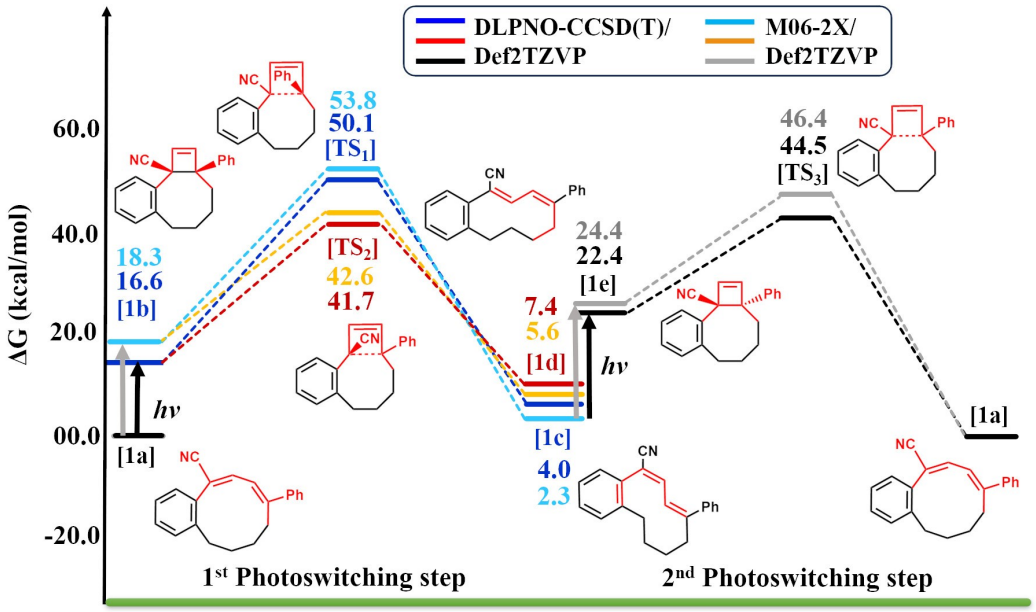

In presence of water

Figure S3. Gibbs free energy profile for thermal electrocyclic ring opening generated relative to the energy of the parent diene **1a**. (a) Energetics calculated in gas phase, and (b) Energetics computed in the presence of water as solvent.

Table S2. The calculated free energy of activation ($\Delta G^{\ddagger}$), reaction energies (ΔG), rate constants (k) and the half-life (τ) of the metastable photoproducts in the gas phase and in the presence of water at both the DLPNO-CCSD(T)/Def2TZVP and M06-2X/Def2TZVP levels of theory.

Method	$\Delta G^{\ddagger}$ (kcal/mol)	ΔG (kcal/mol)	k (s^{-1})	τ (days)
		1b to 1c		
M06-2X (Gas)	34.8	-17.1	1.87×10^{-13}	4.29×10^{7}
DLPNO-CCSD(T) (Gas)	33.4	-13.1	1.99×10^{-12}	4.03×10^{6}
M06-2X (Water)	35.5	-16	5.73×10^{-14}	1.40×10^{8}
DLPNO-CCSD(T) (Water)	33.5	-12.5	1.68×10^{-12}	4.78×10^{6}
		1b to 1d		
M06-2X (Gas)	25.2	-12.3	2.05×10^{-06}	3.91
DLPNO-CCSD(T) (Gas)	25.7	-8.8	8.82×10^{-07}	9.10
M06-2X (Water)	24.3	-12.7	9.38×10^{-06}	8.55
DLPNO-CCSD(T) (Water)	25.1	-9.2	2.43×10^{-06}	3.30
		1e to 1a		
M06-2X (Gas)	22.1	24.9	3.57×10^{-08}	2.25×10^{2}
DLPNO-CCSD(T) (Gas)	21.5	22.2	9.82×10^{-08}	8.17×10^{1}
M06-2X (Water)	22.0	24.4	1.53×10^{-08}	5.23×10^{2}
DLPNO-CCSD(T) (Water)	22.1	22.5	2.15×10^{-08}	3.73×10^{2}

S VII. Docking and Dynamics simulations

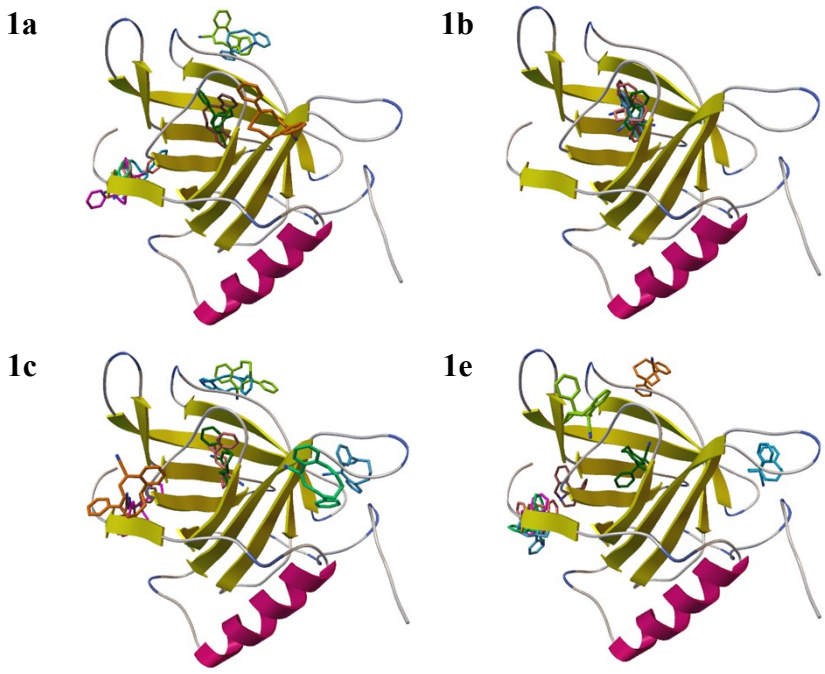

Figure S4. The different binding poses of the photoisomers obtained on the β-barrel protein during the *in silico* molecular docking simulations.

The photoisomer **1b** is observed to occupy only the internal cavity of the β-barrel protein whereas, the other studied photoisomer **1a**, **1c**, and **1e** tends to bound at various sites on the β-barrel protein. Among the various binding poses obtained during the *in silico* molecular docking simulations, molecular dynamics simulations of photoisomer-protein complex were initiated by considering the binding pose having highest magnitude of binding affinity value with the β-barrel protein. It has been noticed that the docking poses of the photoisomers in the internal cavity of the protein have the largest magnitude of the binding affinity values.

Amino acid residues at the binding sites interacting with the photoisomers in the complexes obtained after 150ns of MD simulations

Table S3. The amino acids interacting with the photoisomers bound at the internal cavity of the β-barrel protein in the complexes obtained at 150 ns of the molecular dynamics simulations.

Photoisomers	Interacting amino acids at the binding pocket of β-barrel protein
1a	**Carbon Hydrogen bonding:** ASP31 (2.99) **π Alkyl:** PRO32 (3.87), ALA43 (4.70), ALA55 (3.95), ALA57 (3.96), PHE135 (3.35)

	van der Waals: PHE36 (3.33), TYR90 (3.79), GLN98 (3.91), TYR133 (3.54)
1b	**Carbon Hydrogen bonding:** HIS104 (3.01) **π Alkyl:** PRO32 (3.54), ALA43 (3.55), ALA55 (3.42), ALA57 (3.73), MET73 (3.72) **van der Waals:** PHE36 (3.07), PHE45 (3.23), TYR90 (3.37), TYR133 (3.59), PHE135 (3.88), PHE137 (3.86)
1c	**π-π Stacking:** PHE77 (3.41), PHE135 (3.59) **π Alkyl:** ALA26 (4.01), ILE41 (3.89), ALA55 (3.89) **Pi-Sulfur:** MET73 (3.71), MET88 (3.84) **van der Waals:** PHE36 (3.69), ALA57 (3.86), TYR90 (3.78), PHE137 (3.89)
1e	**Carbon Hydrogen bonding:** HIS104 (3.30) **π Alkyl:** LEU37 (3.54), ILE41 (3.32), ALA55 (3.90), ALA57 (3.57), MET73 (3.96), PHE135 (3.36) **van der Waals:** PHE45 (3.75), LEU37 (3.81), TYR133 (3.85), PHE137 (3.86)

S VIII. REFERENCES

(1) Trott, O.; Olson, A. J. AutoDock Vina: Improving the Speed and Accuracy of Docking with a New Scoring Function, Efficient Optimization and Multithreading. *J Comput Chem* **2010**, *31* (2), 455–461. https://doi.org/10.1002/jcc.21334.

(2) Morris, G. M.; Huey, R.; Lindstrom, W.; Sanner, M. F.; Belew, R. K.; Goodsell, D. S.; Olson, A. J. AutoDock4 and AutoDockTools4: Automated Docking with Selective Receptor Flexibility. *Journal of Computational Chemistry* **2009**, *30* (16), 2785–2791. https://doi.org/10.1002/jcc.21256.

(3) Salentin, S.; Schreiber, S.; Haupt, V. J.; Adasme, M. F.; Schroeder, M. PLIP: Fully Automated Protein-Ligand Interaction Profiler. *Nucleic Acids Res* **2015**, *43* (W1), W443-447. https://doi.org/10.1093/nar/gkv315.